

THE STRUCTURE OF SMOOTH-WALLED SHEAR FLOWS

A.E. PERRY, S.M. HENBEST, K.L. LIM AND M.S. CHONG

DEPARTMENT OF MECHANICAL ENGINEERING

UNIVERSITY OF MELBOURNE, PARKVILLE, VIC. 3052 AUSTRALIA

Using the attached eddy hypothesis of Townsend (1976) and the model of wall turbulence proposed by Perry & Chong (1982), the spectral similarity laws for streamwise, normal and lateral velocity fluctuations are derived. These are compared with measured experimental data. The agreement between the experimental data and the deduced scaling laws is encouraging.

INTRODUCTION

Perry & Chong (1982) proposed a model for wall turbulence which was based on Townsend's (1976) attached eddy hypothesis. Using the observations of Head and Bandyopadhyay (1981) as a guide, wall turbulence was modelled as a "forest" of hair-pin or "A" shaped vortices attached to the boundary. The vortex filaments originate from viscous sublayer material.

It was proposed that a range of scales of geometrically similar "forests" exist and that each "forest" or hierarchy has the same characteristic velocity scale (which is the wall shear velocity U_1). The length scales of the hierarchies range from the scale of the smallest eddies at the wall which have the Kline (1967) scaling δ_1 to the largest scale which is taken to be the pipe radius or the boundary layer thickness Δ_E . Two different probability density functions (p.d.f.'s) of hierarchy scales were tested. One was a discrete distribution with the scales going in a geometric progression and the other was a continuous distribution and was of inverse power law form as assumed by Townsend (1976). It was found that both distributions give much the same result. How the hierarchies are formed is not understood. Nevertheless, such a model gives the correct mean flow velocity distribution. Also using the velocity signatures generated by such an ensemble of vortex filaments with the aid of the Biot-Savart law, it appears that the correct spectral distribution for the streamwise velocity fluctuations u_1 is obtained. The power spectral density for u_1 is characterized by a flat region at low wavenumbers which asymptotes into a -1 power law which then asymptotes into an exponential-like curve at high wavenumbers. Perry & Chong's (1982) analysis was rather crude and the velocity fluctuations u_3 normal to the wall were not considered. This paper outlines a more refined approach to the problem and presents some new data. This new work adds considerable weight to the validity of the theory presented by Perry & Chong.

SPECTRA AND EDDY INTENSITY FUNCTIONS

The analysis of Perry & Chong (1982) was rather crude. The velocity signatures from an isolated vortex "rod" with solid body rotation surrounded by irrotational fluid were used to obtain an ensemble averaged power spectral density for u_1 for a given hierarchy. These densities were then summed up for varying numbers of hierarchies. The resulting spectra appeared to have the correct functional forms when compared with the experimental results of Perry & Abell (1975, 1977) for flow in a smooth-walled pipe.

More refined models are currently being considered by the authors. Unfortunately these are analytically intractable and so numerical methods have

to be used. Figure 1 shows an isolated A-vortex at a boundary with its image vortex. This will be taken to be a "representative eddy" for a given hierarchy.

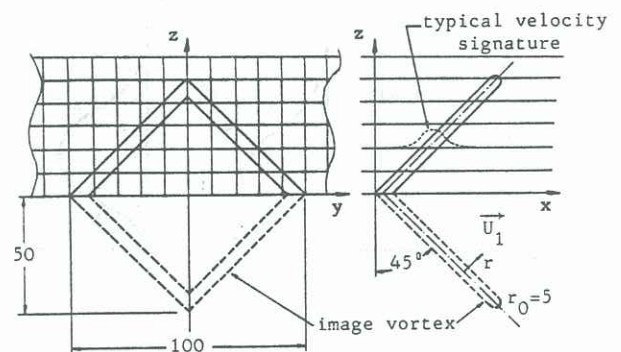


FIGURE 1. A "representative eddy" with streamwise "cuts".

The proportions of the eddy are shown together with the streamwise "cuts" along which u_1 , u_2 and u_3 velocity signatures are generated using the Biot-Savart law. A Gaussian distribution of vorticity is assumed for the vortex "rods" which is

$$\Omega \sim \exp[-(r/r_0)^2/2] \quad (1)$$

where Ω is the modulus of the vorticity at radius r and r_0 is a length scale of the vorticity distribution. (Throughout this paper \sim means 'proportional to' or 'scales with'). The square of the modulus of the Fourier transforms of the u_1 , u_2 and u_3 signatures of this isolated A-vortex is determined and ensemble averaged over each value of z , i.e. we obtain $F_{ii}(k_1, z, z/\delta)$ where k_1 is the streamwise wavenumber and δ is the height of the eddy representative of the hierarchy under consideration. Given that in each hierarchy the average longitudinal and lateral spacings each scale with δ , then the power spectral density $\phi_{ii}(k_1, z)$ for the u_i signatures is given by

$$\phi_{ii}(k_1, z) \sim \int_{\delta_1}^{\Delta_E} F_{ii}(k_1, z, z/\delta) p_H(\delta) d\delta \quad (2)$$

where $\phi_{ii}(k_1, z)$ is the energy per unit non dimensional wavenumber $k_1 z$, δ_1 is the scale of the smallest eddies (i.e. the Kline scaling given earlier) and $p_H(\delta)$ is the

pdf of hierarchy scales. Δ_E is the length scale of the largest hierarchy and this should scale with the shear layer thickness or pipe radius. Assuming a continuous distribution of hierarchy scales then

$$P_H(\delta) \sim \frac{1}{\delta} \quad (3)$$

as used by Townsend. Also it can be shown that

$$\int_0^\infty F_{ii}(k_1 z, z/\delta) d(k_1 z) \sim I_{ii}(z/\delta) \quad (4)$$

where $\Phi_{ii}(z/\delta)$ is the Townsend eddy intensity function I_{ii} (Townsend 1976, pp. 153-155). The authors have not yet included the effect of vortex stretching mentioned by Perry & Chong (1982) but the results so far indicate that the spectra for u_1 fluctuations are much the same as given by the crude analysis of Perry & Chong. Also the spectra for the u_2 and u_3 fluctuations are much the same in functional form as the u_1 fluctuations if we consider only one hierarchy. Figure 2 shows sketches of the eddy intensity functions.

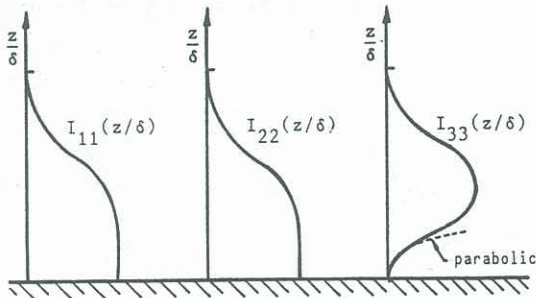


FIGURE 2. Eddy intensity functions.

It should be noted that I_{11} and I_{22} are similar in shape but I_{33} has a different shape as a consequence of the boundary conditions at the wall. Thus we would expect that spectra for u_3 fluctuations to differ considerably from the u_1 and u_2 spectra.

From work carried with simple discrete pdf's (as used by Perry & Chong) the authors expect that equations (2), (3) and (4) and figure 2 will lead to the various spectral similarity regions for u_1 fluctuations as follows.

The "outer flow" similarity law is given by

$$\frac{\Phi_{11}(k_1 \Delta_E)}{U_\tau^2} = G_{11}(k_1 \Delta_E) ; k_1 \leq \frac{M}{z} \quad (5)$$

where $\Phi_{11}(k_1 \Delta_E)$ is the energy per unit non-dimensional wavenumber $k_1 \Delta_E$. For a given large scale flow geometry G_{11} is a universal function. M is a universal constant for all smooth wall flow regions.

The "inner flow" similarity law is given by

$$\frac{\Phi_{11}(k_1 z)}{U_\tau^2} = g_{11}(k_1 z) ; k_1 \geq \frac{B}{\Delta_E} \quad (6)$$

where g_{11} is universal for a smooth wall provided $\delta_1 \ll z \ll \Delta_E$ and B is a constant for a given large scale flow geometry.

Perry and Abell (1977) referred to the motions given by equation (6) as the "universal wall motions". There exists a region of overlap between equations (5) and (6). It can be shown by dimensional arguments that in this region the equations are of the form

$$\frac{\Phi_{11}(k_1 \Delta_E)}{U_\tau^2} = \frac{A_{u1}}{k_1 \Delta_E} ; \frac{B}{\Delta_E} \leq k_1 \leq \frac{M}{z} \quad (7)$$

$$\frac{\Phi_{11}(k_1 z)}{U_\tau^2} = \frac{A_{u1}}{k_1 z}$$

which corresponds to the inverse power law region of the spectrum for u_1 fluctuations mentioned earlier. This inverse power law distribution is a consequence of having a sufficiently large range of hierarchy scales.

A similar behaviour can be shown for the spectra for u_2 fluctuations by virtue of the fact that I_{11} and I_{22} are of similar shape. However, for the spectra of the u_3 fluctuations, only one region of similarity exists, i.e.

$$\frac{\Phi_{33}(k_1 z)}{U_\tau^2} = h_{33}(k_1 z) \quad (8)$$

for all $k_1 z$. The reason for this differing behaviour can be seen from figure 3.

As seen in figure 3(a), a hot-wire probe distant z from the wall "sees" u_1 fluctuations from all eddies whose height δ is of order z and above. Eddies smaller than z are not "seen" by the probe and they do not contribute to the spectrum. Therefore, the resulting

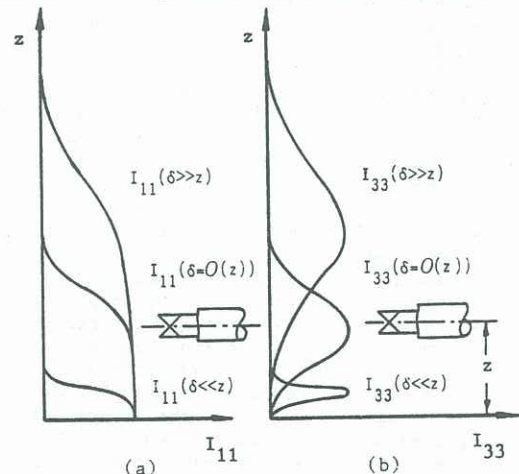


FIGURE 3. (a) I_{11} for various z/δ . (b) I_{33} for various z/δ .

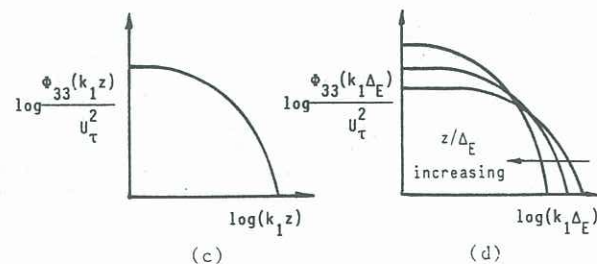
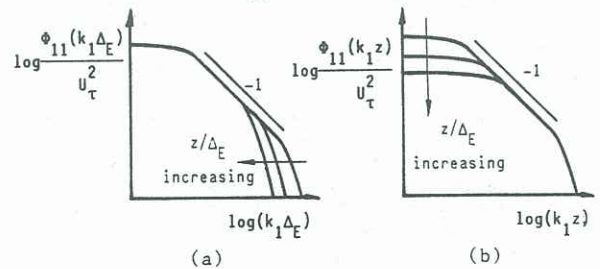


FIGURE 4. "Inner flow" and "outer flow" scaling for u_1 and u_3 spectra for various values of z/Δ_E .

spectrum is made up contributions of all eddies whose scale fall in the range z to Δ_E . On the other hand, as shown in figure 3(b) a probe "sees" u_3 fluctuations only from eddies whose scale is of order z .

Figure 4 shows the various spectra collapsed according to the various similarity laws mentioned above.

EXPERIMENTAL RESULTS

Figure 5 shows the u_1 fluctuation results obtained in a smooth-walled pipe using a 1.26 mm long normal wire.

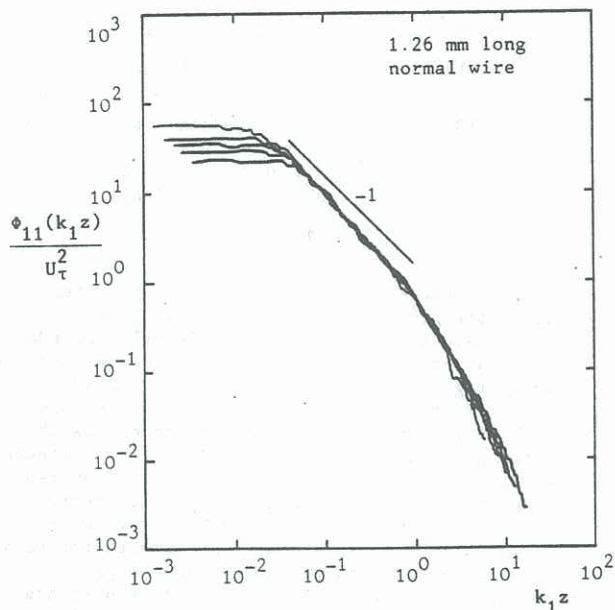


FIGURE 5. "Inner flow" scaling for u_1 spectra for various values of z/Δ_E using a 1.26 mm long normal wire. $Re=200,000$ ($2\Delta_E U_0/\nu$) and $140U_\tau/\nu \leq z \leq 0.14\Delta_E$.

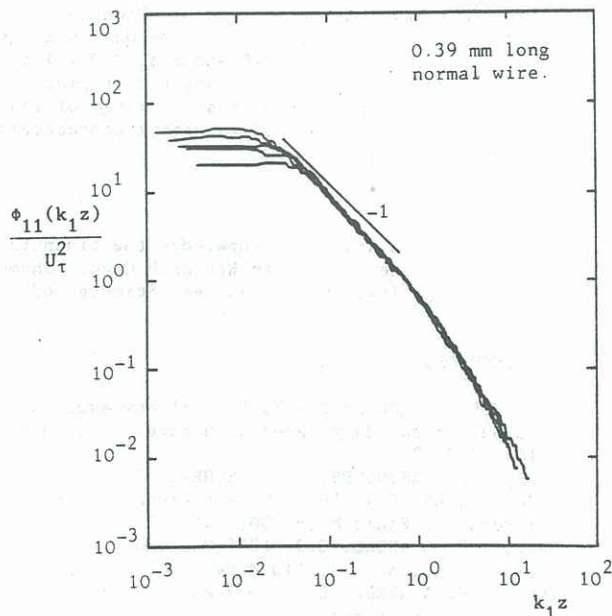


FIGURE 6. "Inner flow" scaling for u_1 spectra for various values of z/Δ_E . $Re=200,000$; 0.39 mm long normal wire and $140U_\tau/\nu \leq z \leq 0.14\Delta_E$.

U_0 is the centerline mean velocity and ν is the kinematic viscosity of the fluid.

Using "inner flow" scaling, one expects the spectra to collapse to an inverse power law and asymptote to an exponential-like curve at high wavenumbers and to "peel-off" from the inverse power law at low wavenumbers for differing values of z/Δ_E , as shown in figure 4(b). The results in figure 6 appear to behave correctly at low and moderate $k_1 z$, however, at high $k_1 z$ they "peel-off" for varying values of z/Δ_E . The smaller the value of z/Δ_E , the earlier the "peel-off" occurs. It appears that as z/Δ_E decreases, the contribution to the spectrum from the smaller hierarchies, whose scale is of order z , decreases and these hierarchies seem to "disappear". One possible reason for the "missing" hierarchies is the spatial resolution limit of the normal wire. This is strongly supported from the data in figure 6 where a 0.39 mm long normal wire was used. One can see some of the "missing" small scale hierarchies have emerged and the data now collapses more convincingly at high wavenumbers and the spectral distribution correlates better with figure 4(b). Figure 7 shows this data using "outer flow" scaling. The collapse at low wavenumbers has improved and the spectra appear to correlate with the scheme shown in figure 4(a)

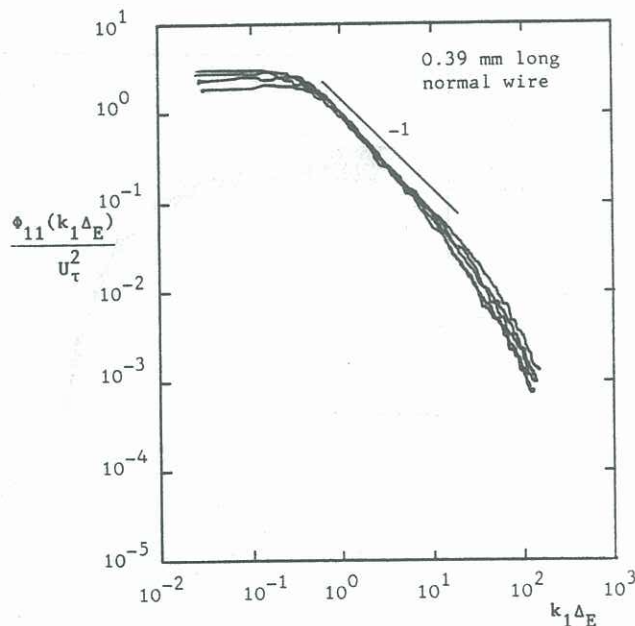


FIGURE 7. "Outer flow" scaling for u_1 spectra for various values of z/Δ_E . $Re=200,000$; 0.39 mm long normal wire and $140U_\tau/\nu \leq z \leq 0.14\Delta_E$.

Figures 8 and 9 show the u_3 fluctuation spectra according "inner flow" and "outer flow" similarity scaling. It can be seen that a more uniform collapse occurs using "inner flow" scaling and that the spectral shape is characteristic of one hierarchy. (i.e. no inverse power law occurs). However, at high wavenumbers the spectra successively "peel-off" earlier for decreasing values of z/Δ_E . Once again, this is most probably a spatial resolution effect. As z/Δ_E decreases the scale of the X-wires increases relative to the scale of the hierarchy which contributes to u fluctuations, which is of order z (see figure 3(b)), and the "observed" contribution to the u_3 spectra at high wavenumbers decreases. The authors propose that if the scale of the X-wires was significantly reduced, the spectra obtained would collapse to a universal curve for all $k_1 z$ as shown in figure 4(c).

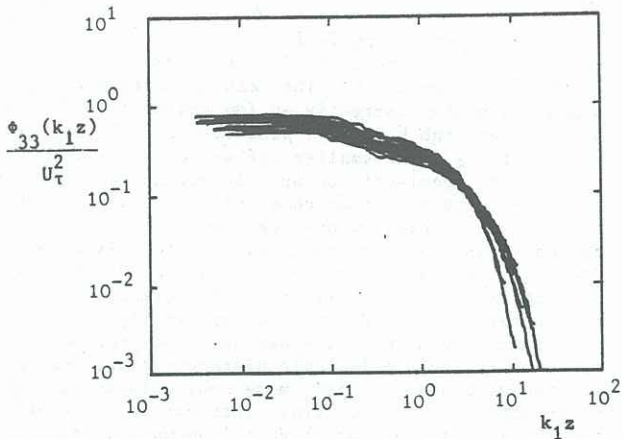


FIGURE 8. "Inner flow" scaling for u_3 spectra for various values of z/Δ_E .
 $Re=75,000$ to $200,000$ and
 $140U_\tau/\nu \leq z \leq 0.14\Delta_E$.

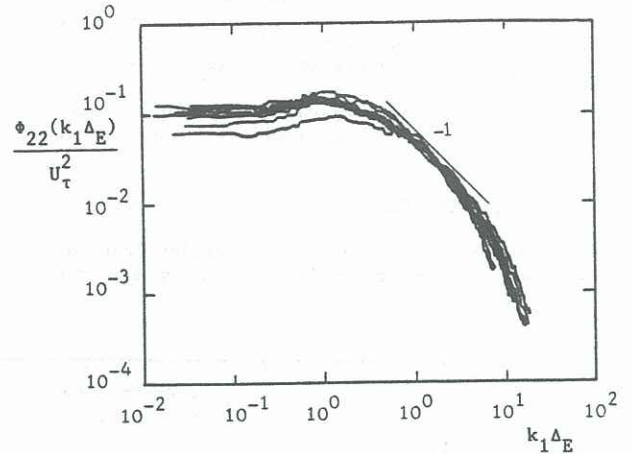


FIGURE 11. "Outer flow" scaling for u_2 spectra for various values of z/Δ_E .
 $R_\theta=5,130$ to $11,880$ and
 $140U_\tau/\nu \leq z \leq 0.14\Delta_E$.

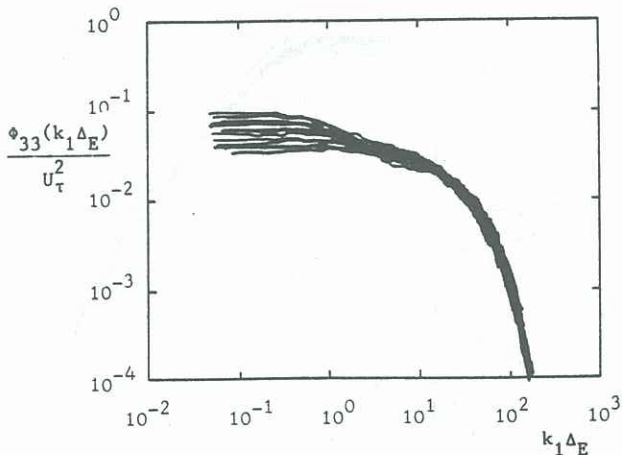


FIGURE 9. "Outer flow" scaling for u_3 spectra for various values of z/Δ_E .
 $Re=75,000$ to $200,000$ and
 $140U_\tau/\nu \leq z \leq 0.14\Delta_E$.

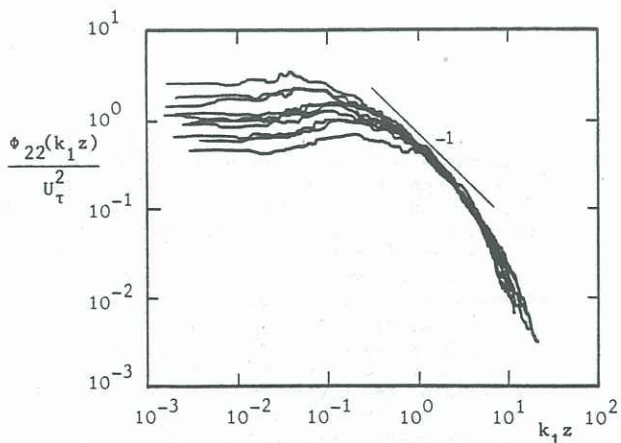


FIGURE 10. "Inner flow" scaling for u_2 spectra for various values of z/Δ_E .
 $R_\theta=5,130$ to $11,880$ ($R_\theta=U_0\theta/\nu$);[†]
 $140U_\tau/\nu \leq z \leq 0.14\Delta_E$.

[†] θ is the momentum thickness and here U_0 is taken to be the freestream velocity.

Unfortunately, no u_2 results have yet been obtained for pipe-flow. However, some u_2 spectra have been obtained for smooth-walled flat-plate boundary-layer in a zero pressure gradient. These results are shown in figures 10 and 11 using "inner flow" and "outer flow" scaling. One would expect these spectral results to follow a similar scaling scheme as the u_1 spectra, as shown in figures 4 (a) and (b). Although no substantial region corresponding to an inverse power exists, it is encouraging that the spectra collapse at low wavenumbers when "outer flow" scaling is used and "peel-off" at high wavenumbers for varying values of z/Δ_E ; and appear to collapse high wavenumbers when "inner flow" scaling is used and "peel-off" at low wavenumbers for varying values of z/Δ_E . Once again, the lack of collapse in figure 10 at very high wavenumbers is attributed to the spatial resolution limit of the X-wires.

CONCLUSIONS

By comparing spectra for streamwise, normal and lateral velocity fluctuations in the "constant stress layer" close to the wall (i.e. in the wall similarity region defined by $zU_\tau/\nu \geq 140$ and $z/\Delta_E \leq 0.14$) the attached eddy hypothesis is strongly confirmed and so also is the idea that there exists a range of scales of geometrically similar eddies with a characteristic velocity scale given by U_τ .

ACKNOWLEDGEMENTS

The authors wish to acknowledge the financial assistance of the Australian Research Grant Scheme and the Australian Institute of Nuclear Science and Engineering.

REFERENCES

- HEAD, M.R. & BANDYOPADHYAY, P. 1981 New aspects of turbulent boundary-layer structure. *J. Fluid Mech.* 107, 297-337.
- KLINE, S.J., REYNOLDS, W.C., SCHRAB, F.A. & RUNSTADLER, P.W. 1957 The structure of turbulent layers. *J. Fluid Mech.* 30, 741-773.
- PERRY, A.E. & ABELL, C.J. 1975 Scaling laws for pipe flow turbulence. *J. Fluid Mech.* 67, 257-271.
- PERRY, A.E. & ABELL, C.J. 1977 Asymptotic similarity of turbulent structures in smooth- and rough-wall pipes. *J. Fluid Mech.* 79, 785-799.
- PERRY, A.E. & CHONG, M.S. 1982 On the mechanism of wall turbulence. *J. Fluid Mech.* 119, 173-217.
- TOWNSEND, A.A. 1976 "The structure of turbulent shear flow", 2nd edn. Cambridge University Press.